Journal of Luminescence 194 (2018) 641–648

Contents lists available at ScienceDirect

Journal of Luminescence

journal homepage: www.elsevier.com/locate/jlumin

The role of Ti in charge carriers trapping in the red-emitting Lu_2O_3:Pr,Ti phosphor

P. Bolek[a], D. Kulesza[a], A.J.J. Bos[b], E. Zych[a,*]

[a] Faculty of Chemistry, University of Wroclaw, 14. F. Joliot-Curie Street, 50-383 Wroclaw, Poland
[b] Delft University of Technology, Faculty of Applied Sciences, Dep. of Radiation Science and Technology (FAME-LMR), Mekelweg 15, 2629 JB Delft, The Netherlands

ARTICLE INFO

Keywords:
Energy storage
Carriers trapping
Storage phosphors
VRBE
Lu_2O_3:Pr,Ti

ABSTRACT

Lu_2O_3:Pr,Ti storage phosphors were prepared by means of high temperature (1700 °C) sintering both in a reducing atmosphere of the N_2-H_2 mixture (3:1 by volume) and in ambient air. Their thermoluminescent (TL) properties were presented and discussed. Pr singly-doped material showed only very inefficient TL. Ti co-doping boosted the TL efficacy, and the most potent TL was observed for ceramics containing 0.05 mol% of Pr and 0.007 mol% of Ti and made in the reducing atmosphere. Samples prepared in air produced noticeably less intense TL. The glow curves of both materials consisted of one broad asymmetric band with the maximum around 357 °C for the heating rate of 4.7 °C/s. The glow peaks could be fitted with three (reduced samples) or two (air-sintered) components. The latter lacked the high-temperature part of TL compared to the former. T_{max}-T_{stop} experiments indicated that the TL is connected with continuous distribution of trap depths, which were estimated to cover the range of ~ 1.7 to 2.3 eV, and their specific values were slightly dependent on the methodology. Anomalous dependence of the TL intensity on the heating rate made the semi-localized transition the likely mechanism affecting the TL properties of Lu_2O_3:Pr,Ti ceramics. The collected data allowed to construct vacuum referred binding energy (VRBE) level scheme with Pr^{3+} and $Ti^{3+/4+}$ energy levels in the band gap of Lu_2O_3 host that could explain the TL mechanism in Lu_2O_3:Pr,Ti ceramics.

1. Introduction

Persistent luminescent and storage phosphors/dosimeters form a unique class of luminescent materials whose physics is probably still the least understood among all phosphor materials nowadays [1–5]. Consequently, practically all the practically utilized materials – in environmental, personal or medical dosimetry, computed radiography, bioimaging etc. – were discovered by chance rather than by deliberate research. Nevertheless, last 20 years brought a significant progress in understanding of the mechanisms standing behind energy storage and its controlled, on demand, recovering by means of thermal or optical stimulation. The mentioned progress in this field became possible due to the discovery of new families of persistent luminescent and storage phosphors in the last decade of the XX century and later, and their thorough investigation in many research groups [3,4,6–12]. In this context, a special attention should be given to a semi empirical methodology proposed by Thiel [13,14] and greatly developed by Dorenbos [4,15–19]. This procedure enables to position energy levels of Ln^{3+} and Ln^{2+} ions against valence and conduction bands of the host lattice. This, in turn, permits prediction of electron- or hole-trapping abilities by the Ln ions introduced to the various hosts. Recently, transition metals with empty 3d, 4d or 5d orbitals were also involved and consistent results were obtained [20–22].

While fabrication techniques and parameters are always important for the final product properties, in the case of persistent and storage phosphors they play an extraordinary role [23–25]. Properties of such materials are extremely sensitive to their processing, presence of impurities (intentionally or unintentionally introduced) and their concentrations.

Following a first summary report [26], in this paper we trace and discuss the TL-related processes in Lu_2O_3:Pr,Ti red-emitting ceramic storage phosphor in more detail. This composition falls into a larger family of Lu_2O_3-based storage and persistent luminescent materials [23–25,27–31] on which we reported previously. The experimental data and their analysis presented here gives a greater insight to physics behind the thermoluminescence in this material.

2. Synthesis

The starting powders of Lu_2O_3:Pr,Ti were prepared by the classic

* Corresponding author.
E-mail address: eugeniusz.zych@chem.uni.wroc.pl (E. Zych).

http://dx.doi.org/10.1016/j.jlumin.2017.09.028
Received 29 June 2017; Received in revised form 6 September 2017; Accepted 11 September 2017
Available online 13 September 2017

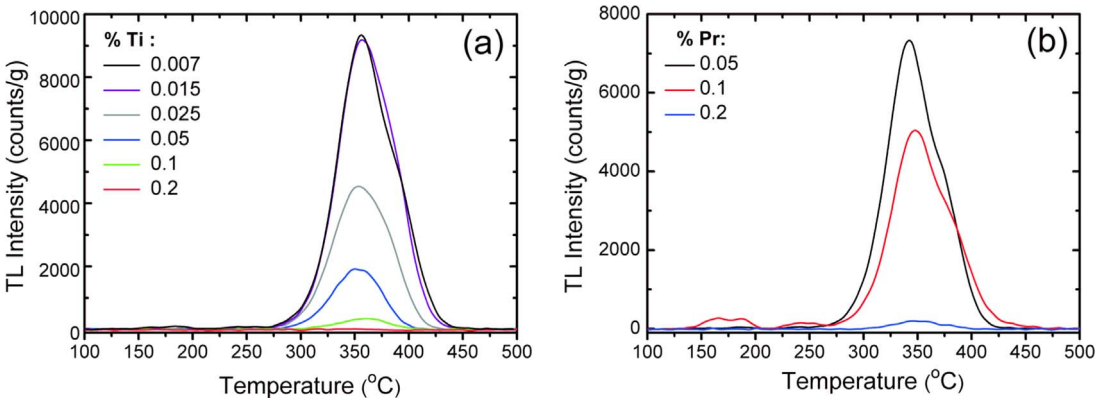

Fig. 1. TL glow curves of Lu_2O_3:Pr,Ti as a function of concentration of titanium when Pr content is 0.05% (a) and TL glow curves as a function of concentration of praseodymium when Ti content is 0.007% (b). Materials were sintered in reducing atmosphere at 1700 °C for 5 h. TL glow curves were registered after exposure of the samples to 254 nm radiation. TL intensity was monitored for the red emission of Pr^{3+}.

Pechini method [32]. Stoichiometric amounts of lutetium(III) nitrate pentahydrate, ($Lu(NO_3)_3{\cdot}5H_2O$, 99.99%), praseodymium(III) nitrate hexahydrate, ($Pr(NO_3)_3{\cdot}6H_2O$, 99.99%) and 1% solution of titanium isopropoxide ($Ti[(OCH)(CH_3)_2]_4$, 99.999%) (in aqueous citric acid solution) were dissolved in 2 M aqueous citric acid solution to complex the metal ions and then ethylene glycol was added to that solution. Next, the mixture was slowly heated up to 100 °C on a hot plate to remove water. Afterwards, the temperature was gradually increased to ~ 600 °C to form resin at first and then burn most of the organics. The final traces of organics were removed by heat-treatment in a chamber furnace at 700 °C for 5 h in air. The obtained powders were white. Portions of about 0.2 g of powders were pressed into pellets 8 mm in diameter under the load of 4 t for 5 min. Each pellet was sintered in a tube furnace in air or in forming gas (75%N_2-25%H_2) at 1700 °C for 5 h in a corundum crucible. A few samples were sintered at lower temperatures to learn more on the role of this parameter on the carries trapping in the investigated compositions. It was shown previously for other Pr,M and Tb,M (M = Hf, Nb, Ti) ceramics that sintering temperature greatly affects their storage capabilities [24,30].

3. Material characterization

The phase purity of all samples was tested by powder X-ray diffraction (XRD) method using a D8 Advance diffractometer from Bruker with Nickel-filtered $CuK_{\alpha 1}$ radiation (λ = 1.540596 A). Measurements were performed in the range of 2θ = 10–80°. TL glow curves were measured using custom-made TL set-up in the range of 25–500 °C with the heating rate of β = 4.7 °C/min. The set-up consisted of a custom made temperature controller allowing for a linear heating, an Ocean Optics HR2000 CG spectrometer operating under the OOIBase dedicated software and 74-UV lens coupled to a QP600-1-SR waveguide which collected and transferred the light emitted by the sample to the CCD detector. The system spectral resolution was about 1.2 nm. Before TL measurements the ceramics were irradiated with 254 nm radiation from a 12 W mercury lamp equipped with a Co filter. TL intensity was monitored for the red emission of Pr^{3+} at 631.5 nm with the bandwidth defined by the resolution of the system estimated to ~ 1.2 nm. The system allowed for a simultaneous recording of the TL emission spectra in the range of 200–1000 nm with 1 s interval. The TL glow curves were fitted using a GlowFit software [33] assuming a first order kinetics of the process. Since the Pr^{3+} luminescence is thermally quenched above room temperature, before fitting the TL glow curves were corrected for the quenching as described in [26]. For thermal partial cleaning (T_{max}-T_{stop}) experiments the ceramics were irradiated with 254 nm radiation for 5 min. Then the specimen was preheating to a specified temperature from the range of 260–360 °C and quickly cooled to RT. Eventually, a regular thermoluminescence experiment was conducted. Fading was registered using RISO TL/OSL reader model DA-15 and controller model DA-20. Sample was irradiated with $^{90}Sr/^{90}Y$ β-source with a dose rate of 0.7 mGy/s. Measurements were performed in nitrogen gas atmosphere with a heating rate of 5 °C/s. Absorption spectra were obtained using Cary 5000 Scan UV–vis–NIR spectrophotometer for raw (non-irradiated) material and after irradiation with 254 nm for 5 min. Photoluminescence excitation (PLE) and emission (PL) spectra of Lu_2O_3:Pr,Ti and Lu_2O_3:Ti samples – raw and after its exposure to UV radiation for 5 min – were recorded using FLS 980 spectrofluorometer from Edinburgh Instruments equipped with a Xenon arc lamp as an excitation source.

4. Results and discussion

XRD patterns of all specimens perfectly agreed with the cubic C-type structure of Lu_2O_3 [34,35]. This was also true for higher dopant contents (up to 2%). Consequently, we assume that both dopants, Pr and Ti, dissolve in Lu_2O_3 host material forming solid solutions. Let us recall that there are two non-equivalent positions of Lu^{3+} ion in the cubic Lu_2O_3 host: centrosymmetric C_{3i} and non-centrosymmetric C_2, whose populations ratio is 1:3 [34,35]. Obviously, the dopants may share between the sites in a ratio to some extent different, as was shown for Eu in the same host [36]. Each Lu atom is placed in the center of a cube whose six corners contain oxygen atoms and two others are empty. These may be easily used to compensate higher charges of dopants, +4, or even +5 [26].

At first, we experimentally recognized the effect of the dopants, Pr and Ti, concentrations as well as the atmosphere of the ceramics fabrication on their TL efficiency. We found, see Fig. 1, that TL efficiency is very much dependent on both Pr and Ti concentrations. In general, high-intensity TL is produced by diluted systems only. When Pr content reached 0.2% TL almost completely disappeared. The TL efficiency was even more sensitive to Ti content, and practically disappeared when Ti concentration reached also 0.2%. It is important that the decay time of photoluminescence (not presented) hardly changes for the investigated concentrations and photoluminescence is very efficient for all investigated concentrations. Thus, the disappearance of TL for higher concentrations is not due to concentration quenching of the luminescence but must be related to decreased ability of carriers trapping rather. Finally, it was found that the TL intensity was the highest for two ceramics Lu_2O_3:0.05%Pr,0.007%Ti and Lu_2O_3:0.05%Pr,0.015%Ti.

The singly activated Lu_2O_3:Pr ceramics, similarly to Lu_2O_3:Tb [27], shows weak TL. It is about two orders of magnitude lower than from the (Pr,Ti) co-doped specimens (compare Fig. 2a and b). Also the shapes of TL glow curves of the singly- and doubly-doped Lu_2O_3 are much different. In the case of the former two low-intensity narrow peaks peaking around 150 °C and 350 °C are present. In contrary, (Pr,Ti) co-doping

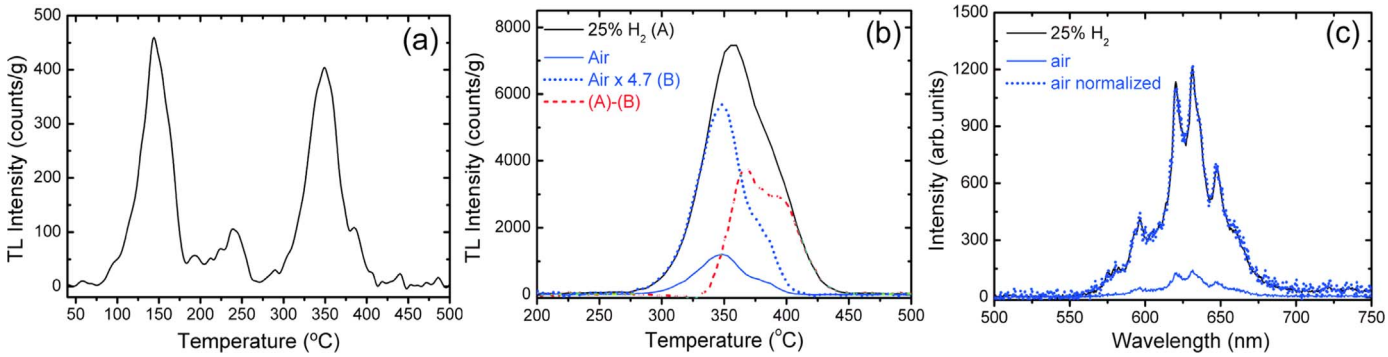

Fig. 2. TL glow curve of Lu_2O_3:0.05%Pr sintered in air atmosphere (a) TL glow curves of Lu_2O_3:0.05%Pr, 0.007%Ti sintered in reducing and in air atmosphere (b) TL emission spectra at 350 °C of Lu_2O_3:0.05%Pr,0.007%Ti ceramics sintered in reducing and air atmosphere (c). (For interpretation of the references to color in this figure legend, the reader is referred to the web version of this article.)

leads to just one broad structured TL component peaking around 355–360 °C. This clearly shows that the Ti co-doping greatly affects the ceramics capabilities of charge carriers trapping, thus the trap parameters and populations.

In Fig. 2b TL glow curves of the Lu_2O_3:0.05%Pr,0.007%Ti ceramics sintered either in reducing (N_2-H_2 mixture, black line) or in oxidizing (air, solid blue line) atmospheres are compared. It is noteworthy that the oxidized sample showed slight brown-yellow coloration, presumably resulting from oxidization of some praseodymium into Pr^{4+}.

A higher TL intensity, by about an order of magnitude, was recorded for the reduced material. Apparently, the reducing atmosphere enhances the population of trapping sites in Lu_2O_3:Pr,Ti. This observation might be rationalized keeping in mind that the high-temperature treatment in oxidized atmosphere certainly convert part of Pr into Pr^{4+}, as these samples were slightly brownish. However, these ions cannot participate in hole trapping. Then, the more efficient carriers trapping in the reduced material has to result from higher concentration of Pr^{3+} ions (h-traps) while still significant fraction of Ti exist as Ti^{4+}. The latter is confirmed by easy recordable its charge transfer luminescence. When the air-sintered ceramics glow curve is multiplied by a factor of 4.7 (blue dotted line in Fig. 2b) its low temperature onset, from 275 °C up to about 335 °C overlays perfectly with the TL glow curve of the reduced specimen. It is then clear that the air-treated ceramics not only shows lower overall TL intensity but it also lacks totally the high-temperature fraction of the reduced ceramics TL. These are depicted by the (differential) red dashed line in Fig. 2b. It gives the difference between the *measured* TL of the reduced specimen (black line) and the *adjusted* (×4.7) TL of the air-sintered ceramics (dotted blue line). By eye, this curve shows two components. The high-temperature one represents TL totally missed in the air-sintered material compared to the reduced one. The other constituent peaking in the differential curve around 370 °C indicates lower efficacy of the related TL in the oxidized ceramics.

In Fig. 2c the TL emission spectra recorded at 350 °C for ceramics sintered in the two different atmospheres are compared. During the experiments the emissions were recorded over 200–1100 nm by CCD camera and exclusively the Pr^{3+} $^1D_2 \rightarrow {}^3H_4, {}^3H_5$ TL luminescence was observed in both ceramics. Since the TL occurs at high temperatures the spectral features are significantly broadened and they form a structured band covering the 570–700 nm range of wavelengths.

In Fig. 3a the charging curve of the Lu_2O_3:Pr,Ti storage phosphor recorded upon 254 nm irradiation is presented. The PL intensity increases continuously during the first ~ 500 s and becomes stable afterwards. Fig. 3b presents a set of TL glow curves recorded after different times of irradiation, thus for different doses. The peak position and shape of the glow curve recorded after 10 s of irradiation is noticeably different than for higher doses. Clearly, at the very early stages of irradiation the charge carriers go to the deeper traps (TL ~ 400 °C) approximately as efficiently as to those giving TL around 350 °C. This makes the glow curve recorded after 10 s of irradiation shifted to higher temperatures with maximum around 368 °C. All other glow curves (taken after higher doses) peaks around 357 °C and the low temperature component roughly doubles the intensity of the high-temperature constituent. Hence, the first-order kinetics is proved.

To get a better insight into the traps structure, we first used the initial rise method [1,2,37–40]. This allowed to estimate the depth of the lowest-temperature trap recording glow curves as a function of irradiation time (dose). Accordingly, fits of the linear parts of the low-temperature onsets of TL glow curves in Arrhenius plots for different doses (see Fig. 3c) allowed to calculate trap depths according to Eq. (1).:

$$I(T) = C \exp\left(\frac{-E_t}{kT}\right), \tag{1}$$

where, C is a constant (includes frequency factor assumed to be independent on the temperature), E_t is trap depth, k is the Boltzmann constant and T is temperature in Kelvin [2]. Inset in Fig. 3c shows trap depths obtained using the initial rise method for the various doses. All the obtained values are very similar and locates between 2.0 and 2.1 eV.

From the presented data it is clear that the TL glow curves are composed of a few strongly overlapping components. The fitting was performed both for the ceramics sintered in forming gas (Fig. 4a) and in air (Fig. 4b). For the reduced material three components were needed while for the air-sintered ceramics it was enough to use two peaks to get a reasonable fit. This accords with the differences of the respective glow curves presented in Fig. 2b. The trap parameters – depths and frequency factors - are given in Table 1 together with lifetimes at RT and at 300 °C calculated according to the Arrhenius function [5] given by Eq. (2):

$$\tau = s^{-1} exp\frac{E}{kT}, \tag{2}$$

where s is frequency factor (s^{-1}), τ is a time a carrier spends in its trap of depth E. It appears that the traps #1 and #2 have very similar parameters (E and s) in both materials (oxidized and reduced). This adheres with the observation made discussing data in Fig. 1b – the low-temperature part of TL in both materials is due to the same type of traps. The trap depths cover the range of 1.7–2.1 eV for reduced specimen and 2.0–2.15 eV for the air sintered one. What is peculiar, however, is that using this method the traps giving TL at lower temperatures were found deeper than those with TL at higher temperatures. Simultaneously, the frequency factors of the traps were also decreasing noticeably from trap #1 to #3 (see Table 1). For the regular first-order kinetics of TL in Lu_2O_3:Pr,Ti the expected value of s would be ~ $1.7 \times 10^{13}\ s^{-1}$, as the cut-off frequency of Lu_2O_3 is ~ 580 cm^{-1} [41]. Thus, the quite different values of s for the various traps, rather high value of s for the first trap and low for the third one (reduced sample) may imply that the TL mechanism may be more complicated and that

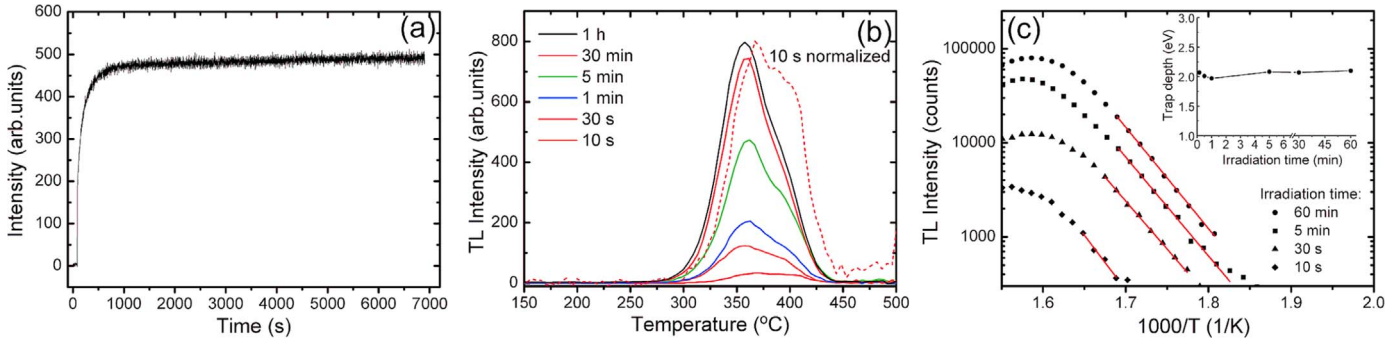

Fig. 3. The charging curve of Lu_2O_3:Pr,Ti recorded upon 254 nm irradiation monitoring 631.5 nm emission (a) Influence of irradiation time with 254 nm radiation on the TL glow curve of Lu_2O_3:Pr,Ti ceramics (b) TL glow curves plotted in Arrhenius diagram and (in inset) estimated trap depths in Lu_2O_3:Pr,Ti for the various irradiation times calculated from the slope of the initial rise range.

the derived trap parameters are good fit parameters but not related to physical quantities.

It was recognized that higher values of *s* may indicate that a semi-localized transition (SLT) plays a role in the TL of Lu_2O_3:Pr,Ti [42–45]. On the other hand, Pagonis showed that TL occurring with the use of common excited state of the hole- and electron-traps upon fitting tend to produce lower-energies for traps producing TL at higher temperatures [46] – exactly as in our case, see Table 1. We shall return to this problem later discussing the proposed model of TL processes in Lu_2O_3:Pr,Ti.

Releasing of trapped charge carriers may be executed not only by thermal, but also (although not in all storage phosphors) by proper optical stimulation. Upon charging the traps in Lu_2O_3:Pr,Ti a broad absorption and excitation bands covering near-UV and bluish-cyan part of spectrum (see Fig. 5a, b) is developed (it partially overlaps with the 4f→5d bands of Pr^{3+}, see Fig. 5b). Evidently, it is connected with the charge carriers trapping. Thus, we also applied controlled optical bleaching into this band to monitor the traps' cleaning. Fig. 5c compares glow curves of freshly irradiated Lu_2O_3:Pr,Ti ceramics with 254 nm and after its subsequent bleaching with either 490 nm or 395 nm radiation. The latter light (~ 3.14 eV) empties the traps completely – the TL is no longer observed. Yet, the 490 nm (2.53 eV) radiation liberates only part of the stored carriers without releasing those giving rise to the high-temperature part of TL, presumably those in trap #3 (Table 1). Thus, the optical stimulation wavelength determines which trapped carriers are released depending on the depth of traps. Let us stress that, whichever the stimulation is, emission comes from Pr^{3+} ions exclusively, as in the case of TL. Accordingly, the broad absorption generated during energy storage (carriers trapping) (Fig. 5a) seems to be a superposition of overlapping components related to traps of different depths. Partial thermal cleaning discussed below will bring more data on the problem of energetic structure of traps in Lu_2O_3:Pr,Ti.

Table 1
Trap parameters derived from fitting of TL glow curves of the Lu_2O_3:Pr,Ti ceramic assuming first-order kinetics together with lifetimes at RT and 300 °C.

Trap #	T (°C)	E (eV)	s (s^{-1})	Lifetime @ RT (years)	Lifetime @ 300 °C (s)
Ceramics sintered in the mixture of H_2-N_2 (Fig. 4a)					
1	350	2.1	$3.0*10^{16}$	$3.5*10^{11}$	100
2	371	1.9	$1.9*10^{14}$	$2.3*10^{10}$	267
3	393	1.7	$1.6*10^{12}$	$1.1*10^{9}$	560
Ceramics sintered in air (Fig. 4b)					
1	345	2.15	$9.9*10^{16}$	$7.4*10^{11}$	82
2	374	2.0	$7.6*10^{14}$	$2.8*10^{11}$	342

For TL bands composed of overlapping components McKeever introduced the so-called T_{max}-T_{stop} method [1,47]. The results for our reduced material are presented in Fig. 6a and the T_{max}-T_{stop} dependence is given in Fig. 6b. Data in Fig. 6b show that up to the T_{stop} = 290 °C the TL peaks are firmly located at ~ 352 °C. This reflects the trap #1 (Table 1) giving rise to the TL at lowest temperatures. However, for T_{stop} > 290 °C the peak position moves continuously to higher temperatures without forming a clear plateau. This is characteristic for a set of traps with very similar parameters (depths) furnishing so called quasi-continuous distribution of trap depths [47]. In the analysis presented in Fig. 4 and Table 1 this complex is indicated by traps #2 and #3 and we shall continue using this terminology.

To learn more about the trap depths, taking advantage of data in Fig. 6a, we employed the initial raise method on partial cleaned glow

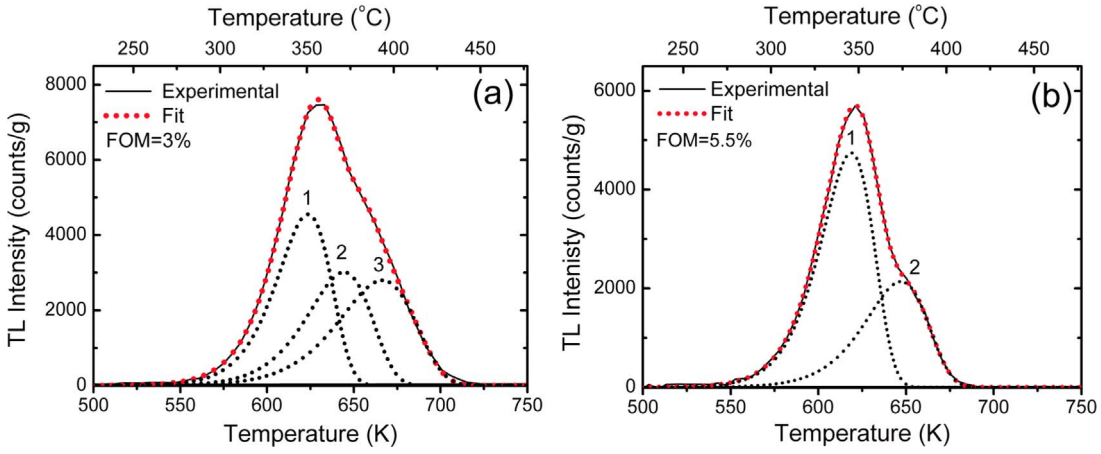

Fig. 4. TL glow curve of Lu_2O_3:Pr,Ti registered after 5 min irradiation of 254 nm radiation (solid line) sintered in a H_2-N_2 mixture (a) and in air (b). Dotted lines show result of first-order kinetic fitting.

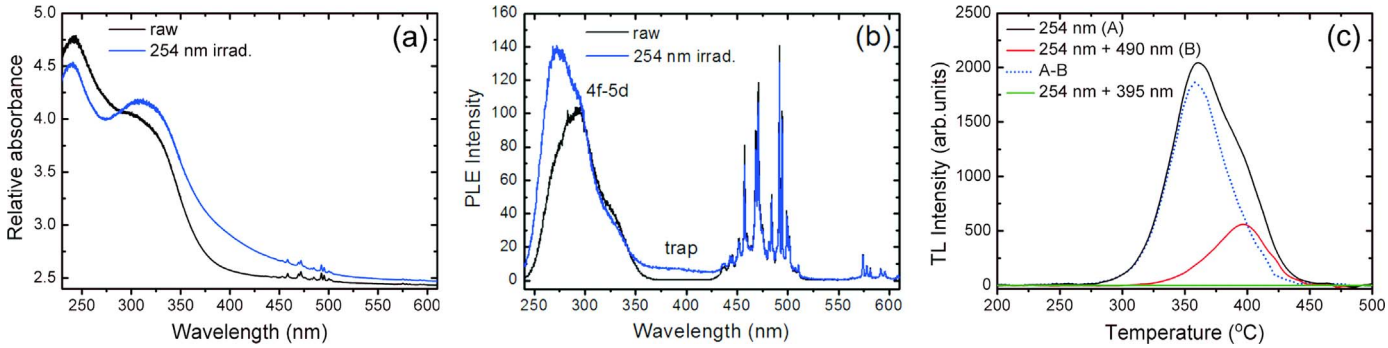

Fig. 5. Changes in absorption (a) and PLE (b) of Lu_2O_3:Pr,Ti upon 254 nm radiation. Changes in TL glow curves due to 3-h optical bleaching with 395 nm or 490 nm radiation (c).

curves [1]. Using this procedure we plotted glow curves in the Arrhenius diagram (Fig. 6c) and calculated the trap depths (according to Eq. (1)). We obtained a group of points with similar energies in the range of 2.1 ± 0.1 eV within the whole range of T_{stop} temperatures (see inset in Fig. 6c). At first it may be implausible that the data produced actually one energy for the whole set of traps – their existence was evidently proved above. Yet, van den Eeckhout et al. [48] investigated the effect of the trap depths distribution on the traps energies obtained using the initial rise method. Their analysis showed that for continuous traps distribution the initial rise procedure actually gives just one trap energy (depth) and its value coincides roughly with the shallower of the traps [40]. Concluding, all the data presented above conform with the concept that in Lu_2O_3:Pr,Ti a continuous distribution of traps contributes to TL and shallowest of them are characterized by depths of ~ 2.0 to 2.1 eV. Nevertheless, we should note that quite similar characteristics as in the inset of Fig. 6c can be observed when localized, thermally activated tunneling process is involved, as was shown for (Lu,Y)AlO_3:Ce [49].

In a regular delocalized Randal-Wilkins mechanism a higher heating rate will cause a shift of the glow peak(s) towards higher temperatures [1]. However, the intensities of TL peaks (when TL/β vs. temperature is plotted) are supposed to be *in*dependent on the heating rate and only their shift to higher temperatures should be seen [42].

Fig. 7 presents TL glow curves (corrected for thermal quenching) of Lu_2O_3:Pr,Ti ceramics taken applying three heating rates (β = 1, 4.7 and 9.1 °C/s). As expected, we observe a shift of the TL maxima towards higher temperatures but, surprisingly, increase of all TL peak intensities with increasing heating rate. This rather rare effect was treated by Mandowski and Bos [42–44] as well as Pagonis [45] in the past. They showed that such a behavior may result from a significant involvement of semi-localized transitions (SLT) through where trapped carriers recombine, presumably non-radiatively, by means of a localized process. Consequently, a low heating rate makes the TL less efficient as then the SLT non-radiative energy dissipation is most significant. Then, with

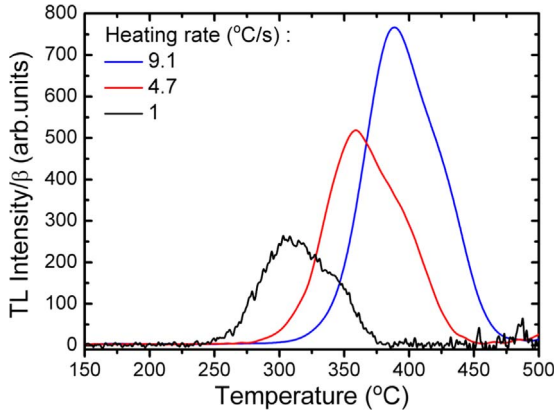

Fig. 7. Corrected for thermal quenching TL glow curves of Lu_2O_3:Pr,Ti registered for various heating rates.

increasing heating rate a growing importance is gaining the regular radiative recombination through the delocalized process in which carriers are liberated to the host conduction/valence band. This is exactly what we see in experiments presented in Fig. 7. Furthermore, since the concentrations of both co-dopants are very low we infer that they show tendency to get spatially correlated (paired) as the SLT needs their interaction, which may occur over limited distances.

In the context of above findings it is important to learn about fading in Lu_2O_3:Pr,Ti ceramics. While the high temperature of TL and large trap depths should lead to negligible fading, the SLT process and deduced tendency for coupling of the co-dopants raise question about their effect on the trapped carriers leakage in time [2]. The results of precise measurements of fading during the first ~ 6.5 h are presented in Fig. 8. Due to a higher sensitivity of the set-up used in these experiments two low-intensity TL components are observed around 150 °C and 230 °C. The fading within the ~ 6.5 h after the irradiation reaches

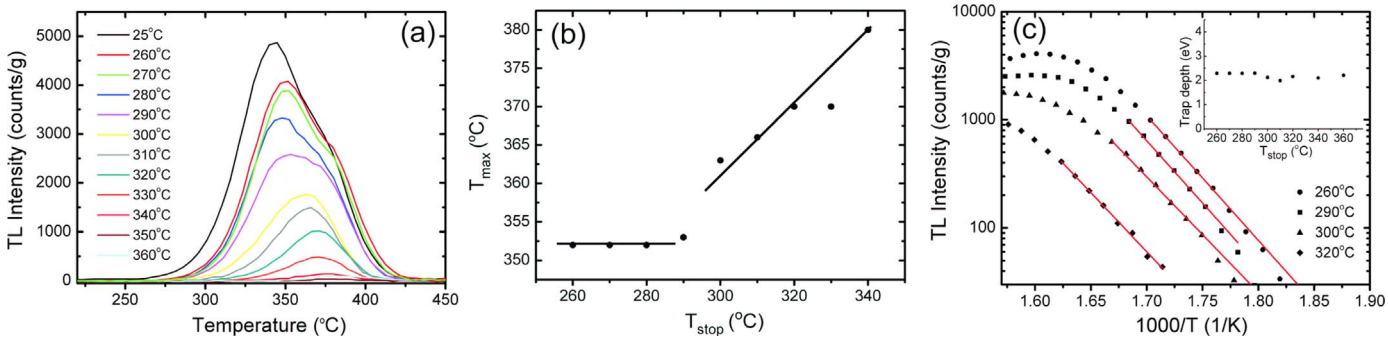

Fig. 6. TL glow curves registered after 5 min of exposure of the ceramic to 254 nm radiation and subsequent preheating to a specified temperature from the 260 to 360 °C range (a) T_{max}-T_{stop} dependence plotted on the basis of the partial thermal cleaning of Lu_2O_3:Pr,Ti glow curve (b) Arrhenius plots of the glow curves registered after thermal cleaning to the 260, 290, 300 and 320 °C (c) and estimated trap depth as a function of T_{stop} obtained using initial rise method combined with partial cleaning (inset).

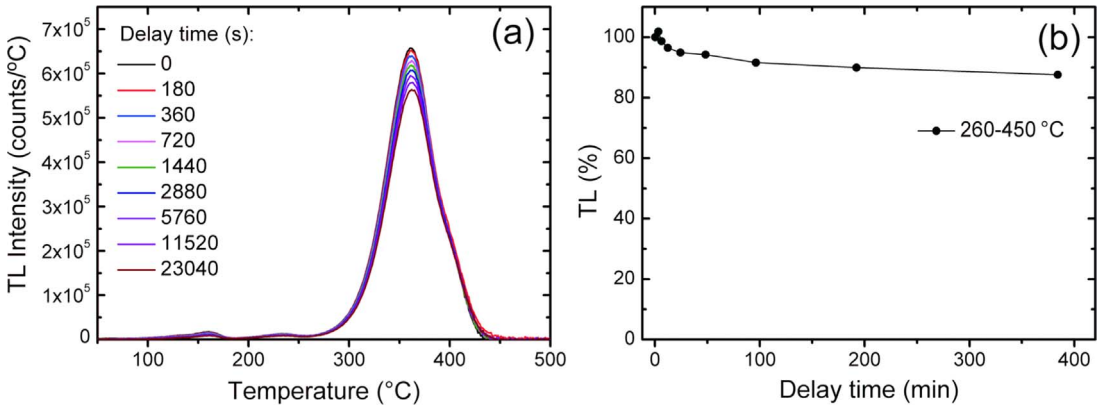

Fig. 8. Fading of TL in Lu_2O_3:Pr,Ti ceramics at RT (a) Decrease of the 260–450 °C band TL (in %) as a function of time (b).

~ 12%. This is more than could be predicted from the trap parameters (see Table 1) and indicates the localized transitions. The leakage is at least partly radiative as we could measure some non-exponentially decaying luminescence from the irradiated sample for a few hours by means of the FLS980 spectrometer. Yet, we should note that even the lowest temperature (~ 150 °C) TL peak lasts till the end of the fading experiments. Thus, the RT afterglow is probably mostly due to this low-temperature TL band. This precludes observation and analysis of fading emission spectrum (or its lack) related exclusively to the most intense high-temperature TL band. So we cannot fully exclude a thermally-assisted tunneling. From Fig. 8b it can be seen that at Room Temperature these transitions have a limited effect on the durability of charge carriers storage in Lu_2O_3:Pr,Ti ceramics. It may be considered a high-temperature TL storage phosphor.

One of the main questions regarding storage or persistent luminescent phosphors is about the charge carriers trapping mechanism and defect sites involved in this process. According to the experimental data presented above, the possible pathways of trapped carriers release in Lu_2O_3:Pr,Ti ceramics are indicated in Fig. 9. Since Pr^{3+}, similarly to Tb^{3+}, is known for its tendency to oxidize to Pr^{4+} it is perfectly reasonable to assume that it serves as a hole trapping center [4,23] at which recombination of carriers occurs in the TL process. Taking into account the glow curves presented in Fig. 2a, b it is reasonable to assume that Ti serves as electron-trapping center.

Taking advantage of the Dorenbos model [21,22,51–53] and spectroscopic data on Lu_2O_3-based phosphors [54–56] a scheme of vacuum referred binding energy (VRBE) of Pr^{3+} electronic levels and Ti^{3+} ground state together with the Lu_2O_3 host valence and conduction bands could be presented in Fig. 9. The position of the Pr^{3+} electronic levels in Lu_2O_3 we determined according to the Dorenbos' model [51]. To position the ground state of the supposed Ti-related electron trap an absorption/excitation spectrum of Lu_2O_3:Ti was needed. Since the samples are not transparent or translucent we have chosen to record its emission and excitation spectra. They are presented in Fig. 10. The emission peaks around 460 nm and is very broad as expected for charge transfer (CT) luminescence. It is composed of two components which seems to reflect the two metal sites of the host lattice. Also the excitation spectrum of Lu_2O_3:Ti shows two bands peaking around 300 nm (4.13 eV) and 265 nm (4.68 eV), which makes the results of these experiments consistent. The PLE bands should be attributed to $O^{2-}\rightarrow Ti^{4+}$ CT transitions, then. Their energies agrees with the recent studies presented by Dorenbos and Rogers [21,22] who found that independently on the host, the energy of $O^{2-}\rightarrow Ti^{4+}$ CT transition is slightly (few tenths eV) lower than energy of analogous $O^{2-}\rightarrow Eu^{3+}$ CT bands. The latter was reported to appear in Lu_2O_3:Eu around 228–238 nm for C_{3i} site and around 245–248 nm for C_2 [55,56]. Thus, our findings are fully consistent with the Dorenbos model. While the presence of two sites in Lu_2O_3 complicates the quantitative analysis the Ti-related electron trap may be reasonably positioned ~ 4.1 eV above the host valence band, as presented in Fig. 9. a is worthwhile to notice that with the positioning of the Ti level with the help of the CT band the trap depths represented by $Ti^{3+/4+}$ e-traps band in Fig. 9 lie between 1.7 and 2.2 eV which is in perfect agreement with the values in Table 1.

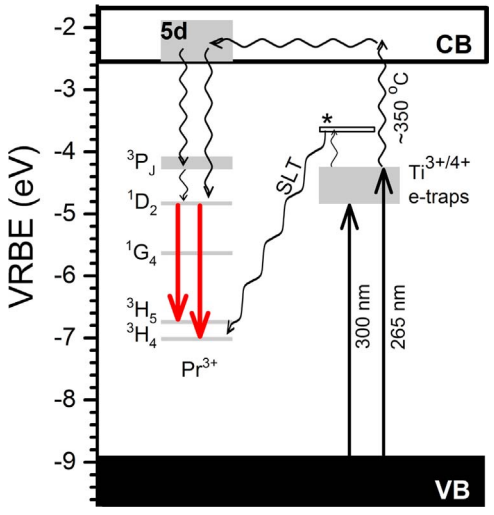

Fig. 9. VRBE level scheme with Pr^{3+} and $Ti^{3+/4+}$ energy levels relative to the Lu_2O_3 host valence and conduction bands. The proposed mechanism of releasing trapped carriers in Lu_2O_3:Pr,Ti ceramics by means of semi-localized transition competing with the regular delocalized process with the use of conduction band is depicted. After Dorenbos [21,50], the $Ti^{3+/4+}$ trap represents the ground state of Ti^{3+} ion attained after trapping an electron by Ti^{4+}.

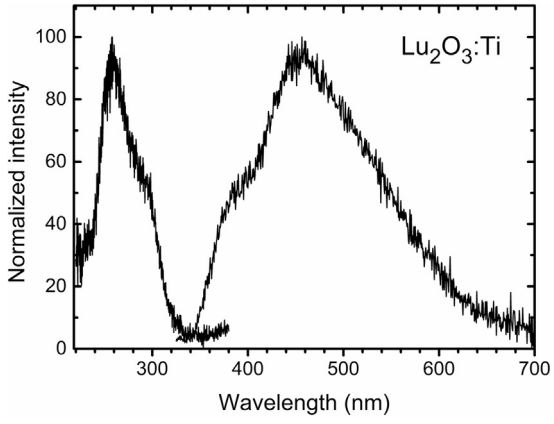

Fig. 10. PLE and PL spectra of Lu_2O_3:Ti ceramics. The emission was excited at 255 nm and for PLE spectrum 450 nm luminescence was monitored.

Thus, all the data appear internally consistent and also correspond quite well quantitatively. Consequently, using the Kröger-Vink notation [57,58], the trapping processes might be described according to Eqs. (3) and (4):

$$Pr^{X}_{Lu} + h^{\bullet} \rightarrow Pr^{\bullet}_{Lu}. \quad (3)$$

$$Ti^{\bullet}_{Lu} + e' \rightarrow Tr^{X}_{Lu}. \quad (4)$$

Upon subsequent heating the electron in Ti^{X}_{Lu} may acquire enough energy to be liberated to the conduction band and diffuse to the $Pr^{\bullet}_{Lu}$ to recombine with the hole trapped there and produce a photon of red light. However, a competitive SLT process appears to occur allowing some of the trapped electrons to fill the hole in $Pr^{\bullet}_{Lu}$ by means of non-radiative SLT process. The occurrence of energy dissipation via the SLT mechanism may be justified by the fact that the Ti^{x}_{Lu} entity, with its similarity to the $O^{2-} \rightarrow Ti^{4+}$ charge transfer state, has to be spatially spread which facilitates interaction of the electron and hole traps over larger distances. This would also explain why higher concentrations of Ti quickly diminishes the TL (= carriers trapping) efficacy, as we earlier mentioned. What is more, the $Ti^{3+/4+}$ entity is expected to have its own $3d^{1}$* excited level denoted with * in Fig. 9, which – according to the theory of SLT transitions – may serve for non-radiative energy flow to $Pr^{\bullet}_{Lu}$, competitive to the regular delocalized (with the use of conduction band) radiative process generating TL. Accordingly, all the observations related to TL of Lu_2O_3:Pr,Ti may be combined into a consistent picture.

What might be considered not fully clear is the presence of continuous traps distribution, which indicates the presence of many electron-traps needing slightly different energies for their electrons to escape This cannot be justified by the two metal sites present in Lu_2O_3 [34,35]. What may differentiate the electron traps is their distance from the $Pr^{\bullet}_{Lu}$ recombination center. By itself it does not change their depths defined as energy needed to reach the bottom of conduction band. Yet, if the transfer of electron from Ti^{X}_{Lu} to $Pr^{\bullet}_{Lu}$ could occur by means of more localized mechanism – with a use of a common excited state for example - the energy needed to overcome the barrier might be then distance-dependent [1,2,59]. While such interactions between Ti^{X}_{Lu} and $Pr^{\bullet}_{Lu}$ trap centers are conceivable and could be considered as versions of intervalence charge transfer interactions [22,60] a further research is needed to verify this hypothesis.

5. Conclusions

Thermoluminescent properties of Lu_2O_3:Pr,Ti ceramics were presented and their ability to efficiently store excited charge carriers was proved. The presence of Ti is crucial for generation of high population of energy trapping sites. From our previous study we know that Pr^{3+} is the recombination center. This study reveals the role of Ti dopant as electron-trapping center. The vacuum referred binding energy levels of trapping centers – Pr^{3+} and $Ti^{3+/4+}$ - were positioned in Lu_2O_3 host. The most efficient TL shows the composition containing 0.05 mol% of Pr and 0.007 mol% of Ti and sintered at high temperatures (1700 °C) in reducing atmosphere of forming gas. Glow curve of Lu_2O_3:Pr,Ti ceramic contains one broad band with maximum around 357 °C. The broad band is the result of a continuous distribution of trap depths present in the storage phosphor. Their activation energies were found to start ~ 2.0 eV. Anomalous dependence of TL intensity on heating rate was demonstrated and explained by semi-localized transition model. Fading of TL was not significant and reached 12% after 6.5 h.

Acknowledgements

The authors gratefully acknowledge financial support by the Polish National Science Centre (NCN) under the Grant #UMO-2014/13/B/ST5/01535.

References

[1] S.W.S. McKeever, Thermoluminescence of Solids, Cambridge University Press, Cambridge, U.K, 1985.
[2] R. Chen, S.W. McKeever, Theory of Thermoluminescence and Related Phenomena, World Scientific Publishing, Singapore, 1997.
[3] A. Lecointre, A. Bessière, A.J.J. Bos, P. Dorenbos, B. Viana, S. Jacquart, Designing a red persistent luminescence phosphor: the example of YPO_4:Pr^{3+},Ln^{3+} (Ln = Nd, Er, Ho, Dy), J. Phys. Chem. C 115 (2011) 4217–4227.
[4] A.J.J. Bos, P. Dorenbos, A. Bessire, A. Lecointre, M. Bedu, M. Bettinelli, et al., Study of TL glow curves of YPO_4 double doped with lanthanide ions, Radiat. Meas. 46 (2011) 1410–1416.
[5] A.J.J. Bos, Theory of thermoluminescence, Radiat. Meas. 41 (2007) 45–56.
[6] H. Yamamoto, T. Matsuzawa, Mechanism of long phosphorescence of $SrAl_2O_4$:Eu^{2+}, Dy^{3+} and $CaAl_2O_4$:Eu^{2+}, Nd^{3+}, J. Lumin. 72–74 (1997) 287–289.
[7] T. Matsuzawa, Y. Aoki, N. Takeuchi, Y. Murayama, A. New Long, Phosphorescent phosphor with high brightness, $SrAl_2O_4$:Eu^{2+},Dy^{3+}, J. Electrochem. Soc. 143 (1996) 2670–2673.
[8] A.H. Krumpel, A.J.J. Bos, A. Bessière, E. Van Der Kolk, P. Dorenbos, Controlled electron and hole trapping in YPO_4: Ce^{3+},Ln^{3+} and LuPO4: Ce^{3+}, Ln^{3+} (Ln = Sm, Dy, Ho, Er, Tm), Phys. Rev. B – Condens. Matter Mater. Phys. 80 (2009) 1–10.
[9] Y. Li, Y. Wang, Y. Gong, X. Xu, M. Zhou, Design, synthesis and characterization of an orange-yellow long persistent phosphor: $Sr_3Al_2O_5Cl_2$:Eu^{2+},Tm^{3+}, Opt. Express 18 (2010) 24853–24858.
[10] H.G. Kang, J.K. Park, J.M. Kim, C.H. Kim, S.C. Choi, Embodiment and luminescence properties of Sr_3SiO_5:Eu (yellow-orange phosphor) by co-doping lanthanide, Solid State Phenom. 124–126 (2007) 511–514.
[11] Y. Gong, Y. Wang, Y. Li, X. Xu, W. Zeng, Fluorescence and phosphorescence properties of new long-lasting phosphor $Ba_4(Si_3O_8)_2$:Eu^{2+}, Dy^{3+}, Opt. Express 19 (2011) 4310–4315.
[12] Y. Miyamoto, H. Kato, Y. Honna, H. Yamamoto, K. Ohmi, An orange-emitting, long-persistent phosphor, $Ca_2Si_5N_8$:Eu^{2+},Tm^{3+}, J. Electrochem. Soc. 156 (2009) 235–241.
[13] C.W. Thiel, H. Cruguel, Y. Sun, G.J. Lapeyre, R.M. Macfarlane, R.W. Equall, et al., Systematics of 4f electron energies relative to host bands by resonant photoemission of rare earth doped optical materials, J. Lumin. 94–95 (2001) 1–6.
[14] C.W. Thiel, R.L. Cone, Investigating material trends and lattice relaxation effects for understanding electron transfer phenomena in rare-earth-doped optical materials, J. Lumin. 131 (2011) 386–395.
[15] A.J.J. Bos, P. Dorenbos, A. Bessière, B. Viana, Lanthanide energy levels in YPO_4, Radiat. Meas. 43 (2008) 222–226.
[16] P. Dorenbos, T. Shalapska, G. Stryganyuk, A. Gektin, A. Voloshinovskii, Spectroscopy and energy level location of the trivalent lanthanides in $LiYP_4O_{12}$, J. Lumin. 131 (2011) 633–639.
[17] P. Dorenbos, E.V.D. Van Loef, A.P. Vink, E. Van Der Kolk, C.W.E. Van Eijk, K.W. Krämer, Level location and spectroscopy of Ce^{3+}, Pr^{3+}, Er^{3+}, and Eu^{2+} in $LaBr_3$, J. Lumin. 117 (2006) 147–155.
[18] T. Shalapska, P. Dorenbos, A. Gektin, G. Stryganyuk, A. Voloshinovskii, Luminescence spectroscopy and energy level location of lanthanide ions doped in La $(PO_3)_3$, J. Lumin. 155 (2014) 95–100.
[19] P. Dorenbos, A.H. Krumpel, E. Van Der Kolk, P. Boutinaud, M. Bettinelli, E. Cavalli, Lanthanide level location in transition metal complex compounds, Opt. Mater. 32 (2010) 1681–1685.
[20] E.G. Rogers, P. Dorenbos, Vacuum referred binding energy of the single 3d, 4d, or 5d electron in transition metal and lanthanide impurities in compounds, ECS J. Solid State Sci. Technol. 3 (2014) R173–R184.
[21] E.G. Rogers, P. Dorenbos, Vacuum energy referred $Ti^{3+/4+}$ donor/acceptor states in insulating and semiconducting inorganic compounds, J. Lumin. 153 (2014) 40–45.
[22] P. Dorenbos, Charge transfer bands in optical materials and related defect level location, Opt. Mater. 69 (2017) 8–22.
[23] J. Trojan-Piegza, J. Niittykoski, J. Hölsä, E. Zych, Thermoluminescence and kinetics of persistent luminescence of vacuum-sintered Tb^{3+} -doped and Tb^{3+},Ca^{2+} -co-doped Lu_2O_3 materials, Chem. Mater. 20 (2008) 2252–2261.
[24] A. Wiatrowska, E. Zych, Lu_2O_3: Pr, Hf storage phosphor: compositional and technological issues, Materials 7 (2014) 157–169.
[25] J. Trojan-Piegza, E. Zych, J. Hölsä, J. Niittykoski, Spectroscopic properties of persistent luminescence phosphors: Lu_2O_3:Tb^{3+}, M^{2+} (M = Ca, Sr, Ba), J. Phys. Chem. C 113 (2009) 20493–20498.
[26] D. Kulesza, P. Bolek, A.J.J. Bos, E. Zych, Lu_2O_3-based storage phosphors. An (in) harmonious family, Coord. Chem. Rev. 325 (2016) 29–40.
[27] D. Kulesza, A. Wiatrowska, J. Trojan-Piegza, T. Felbeck, R. Geduhn, P. Motzek, et al., The bright side of defects: chemistry and physics of persistent and storage phosphors, J. Lumin. 133 (2013) 51–56.
[28] S. Chen, Y. Yang, G. Zhou, Y. Wu, P. Liu, F. Zhang, et al., Characterization of afterglow-related spectroscopic effects in vacuum sintered Tb^{3+}, Sr^{2+} co-doped Lu_2O_3 ceramics, Opt. Mater. 35 (2012) 240–243.
[29] A. Wiatrowska, E. Zych, Traps formation and characterization in long-term energy storing Lu_2O_3:Pr,Hf luminescent ceramics, J. Phys. Chem. C 117 (2013) 11449–11458.
[30] D. Kulesza, E. Zych, Managing the properties of Lu_2O_3:Tb,Hf storage phosphor by means of fabrication conditions, J. Phys. Chem. C 117 (2013) 26921–26928.
[31] D. Kulesza, J. Trojan-Piegza, E. Zych, Lu_2O_3:Tb,Hf storage phosphor, Radiat. Meas. 45 (2010) 490–492.
[32] M. Pechini, Method of Preparing Lead and Alkaline Earth Titanates and Niobates and Coating Method Using the Same to form a Capacitor, US Patent no. 3,330697,

1967.
[33] M. Puchalska, P. Bilski, GlowFit-a new tool for thermoluminescence glow-curve deconvolution, Radiat. Meas. 41 (2006) 659–664.
[34] J. Zeler, Lucjan B. Jerzykiewicz, E. Zych, Flux-aided synthesis of Lu_2O_3 and Lu_2O_3:Eu—single crystal structure, morphology control and radioluminescence efficiency, Materials 7 (2014) 7059–7072.
[35] M. Guzik, J. Pejchal, A. Yoshikawa, A. Ito, T. Goto, M. Siczek, et al., Structural investigations of Lu_2O_3 as single crystal and polycrystalline transparent ceramic, Cryst. Growth Des. 14 (2014) 3327–3334.
[36] G. Concas, G. Spano, E. Zych, J. Trojan-Piegza, Nano- and microcrystalline Lu_2O_3:Eu phosphors: variations in occupancy of C_2 and S_6 sites by Eu^{3+} ions, J. Phys.: Condens. Matter 17 (2005) 2597–2604.
[37] R. Chen, V. Pagonis, Thermally and Optically Stimulated Luminescence: A Simulation Approach, John Wiley & Sons, 2011.
[38] V. Pagonis, G. Kitis, C. Furetta, Numerical and practical Exercises in Thermoluminescence, Springer, New York, 2006.
[39] P. Kivits, H.J. Hagebeuk, Evaluation of the model for thermally stimulated luminescence and conductivity; reliability of trap depth determinations, J. Lumin. 15 (1977) 1–27.
[40] K. Van Den Eeckhout, A.J.J. Bos, D. Poelman, P.F. Smet, Revealing trap depth distributions in persistent phosphors, Phys. Rev. B – Condens. Matter Mater. Phys. 87 (2013) 1–11.
[41] E. Zych, D. Hreniak, W. Strek, Lu2O3:Eu, a new X-ray phosphor, Materials 20 (2002) 111–121.
[42] A. Mandowski, A.J.J. Bos, Explanation of anomalous heating rate dependence of thermoluminescence in YPO_4:Ce^{3+},Sm^{3+} based on the semi-localized transition (SLT) model, Radiat. Meas. 46 (2011) 1376–1379.
[43] A. Mandowski, Semi-localized transitions model-General formulation and classical limits, Radiat. Meas. 43 (2008) 199–202.
[44] A. Mandowski, Semi-localized transitions model for thermoluminescence, J. Phys. D: Appl. Phys. 38 (2005) 17–21.
[45] V. Pagonis, L. Blohm, M. Brengle, G. Mayonado, P. Woglam, Anomalous heating rate effect in thermoluminescence intensity using a simplified semi-localized transition (SLT) model, Radiat. Meas. 51–52 (2013) 40–47.
[46] V. Pagonis, S. Mian, R. Mellinger, K. Chapman, Thermoluminescence kinetic study of binary lead-silicate glasses, J. Lumin. 129 (2009) 570–577.
[47] S.W.S. McKeever, In the analysis of complex thermoluminescence glow-curves: resolution into individual peaks, Phys. Status Solidi 62 (1980) 331–340.
[48] K. Van Den Eeckhout, P.F. Smet, D. Poelman, Persistent luminescence in Eu^{2+}-doped compounds: a review, Materials (2010) 2536–2566, http://dx.doi.org/10.3390/ma3042536.
[49] A. Vedda, M. Martini, F. Meinardi, Tunneling process in thermally stimulated luminescence of mixed $Lu_xY_{1-x}AlO_3$:Ce crystals, Phys. Rev. B 61 (2000) 8081–8086.
[50] H. Luo, A.J.J. Bos, P. Dorenbos, Charge carrier trapping processes in RE_2O_2S (RE = La, Gd, Y and Lu), J. Phys. Chem. C 121 (2017) 8760–8769.
[51] P. Dorenbos, A.J.J. Bos, Lanthanide level location and related thermoluminescence phenomena, Radiat. Meas. 43 (2008) 139–145.
[52] P. Dorenbos, Modeling the chemical shift of lanthanide 4f electron binding energies, Phys. Rev. B – Condens. Matter Mater. Phys. 85 (2012) 1–10.
[53] P. Dorenbos, E.G. Rogers, Vacuum referred binding energies of the lanthanides in transition metal oxide compounds, ECS J. Solid State Sci. Technol. 3 (2014) R150–R158.
[54] E. Zych, J. Trojan-Piegza, Low-temperature luminescence of Lu_2O_3:Eu ceramics upon excitation with synchrotron radiation in the vicinity of band gap energy, Chem. Mater. 18 (2006) 2194–2199.
[55] E. Zych, Concentration dependence of energy transfer between Eu^{3+} ions occupying two symmetry sites in Lu_2O_3, J. Phys.: Condens. Matter 14 (2002) 5637–5650.
[56] E. Zych, A. Meijerink, C.D.M. Doneg, Quantum efficiency of europium emission from nanocrystalline powders of Lu_2O_3: Eu, J. Phys.: Condens. Matter 15 (2003) 5145–5155.
[57] F.A. Kröger, H.J. Vink, Relations between the concentrations of imperfections in crystalline solids, Solid State Phys. – Adv. Res. Appl. 3 (1956) 307–435.
[58] F.A. Kröger, H.J. Vink, In Relations Between the Concentrations of Imperfections in Crystalline Solids in Solid State Physics, Academic Press, San Diego, 1995.
[59] A. Dobrowolska, A.J.J. Bos, P. Dorenbos, Electron tunnelling phenomena in YPO_4:Ce,Ln (Ln = Er, Ho, Nd, Dy), J. Phys. D: Appl. Phys. 47 (2014) 335301.
[60] A.H. Krumpel, E. van der Kolk, E. Cavalli, P. Boutinaud, M. Bettinelli, P. Dorenbos, Lanthanide 4f-level location in $A_VO_{(4)}$:$Ln^{(3+)}$ (A = La, Gd, Lu) crystals, J. Phys. Condens. Matter.: Inst. Phys. J. 21 (2009).